



## *Spirulina* polysaccharide induces the metabolic shifts and gut microbiota change of lung cancer in mice

Yingfang Lu<sup>a,1</sup>, Bo Peng<sup>b,c,1</sup>, Yuqi Lin<sup>a</sup>, Qianmin Lin<sup>a</sup>, Xuwei Xia<sup>a</sup>, Saiyi Zhong<sup>d</sup>, Lianxiang Luo<sup>e,\*</sup>, Riming Huang<sup>a,\*\*</sup>

<sup>a</sup> Guangdong Provincial Key Laboratory of Food Quality and Safety, College of Food Science, South China Agricultural University, Guangzhou, 510642, China

<sup>b</sup> State Key Laboratory of Organic Geochemistry, Guangdong Provincial Key Laboratory of Environmental Protection and Resources Utilization, Guangzhou Institute of Geochemistry, Chinese Academy of Sciences, Guangzhou 510640, China, CAS Center for Excellence in Deep Earth Science, Guangzhou, 510640, China

<sup>c</sup> University of Chinese Academy of Sciences, Beijing, 100049, China

<sup>d</sup> College of Food Science and Technology, Guangdong Ocean University, Guangdong Provincial Key Laboratory of Aquatic Product Processing and Safety, Guangdong Provincial Engineering Technology Research Center of Seafood, Guangdong Province Engineering Laboratory for Marine Biological Products, Key Laboratory of Advanced Processing of Aquatic Product of Guangdong Higher Education Institution, Zhanjiang, 524088, China

<sup>e</sup> The Marine Biomedical Research Institute, Guangdong Medical University, The Marine Biomedical Research Institute of Guangdong Zhanjiang, Zhanjiang, 524000, China

### ARTICLE INFO

Handling Editor: Dr. Quancai Sun

#### Keywords:

*Spirulina*  
Polysaccharide  
Lung cancer  
Metabolomics  
Gut microbiota

### ABSTRACT

A polysaccharide obtained from *Spirulina* (PSP) and its effect on lung cancer in mice was investigated. Our results indicate that the tumor volume and weight of the lung cancer-bearing mice treated with PSP decreased significantly. Metabolite analysis showed that 27 differential accumulated metabolites (DAMs) changed significantly, in which 24 DAMs increased while 3 DAMs decreased. KEGG enrichment results showed that these differential metabolites were enriched significantly in the high-affinity IgE receptor (FcεRI) signaling pathway and arachidonic acid metabolism. In addition, PSP modulated gut microbiota of the lung cancer-bearing mice. PSP increased the abundance of *Lactobacillus*, *Allobaculum*, *Alloprevotella*, and *Olsenella*, decreasing *Bacteroides* and *Acinetobacter*. The results might be related to suppressing lung cancer. Based on our study, we hypothesized that PSP inhibited lung cancer through FcεRI signaling pathway and arachidonic acid metabolism and regulated the balance of gut microbiota. Nevertheless, the relationship between these two pathways and gut microbiota needs further study.

### 1. Introduction

Cancer has been a public health concern worldwide, and although the death rate from cancer has continued to decline since 1991 (Siegel et al., 2019), the annual number of cancer cases remains large. In terms of mortality, cancer deaths remain a severe problem worldwide (8.97 million deaths), only after ischemic heart disease (Bray et al., 2018). Therefore, the cancer problem still needs to be solved. Lung cancer is one of the deadliest cancers (Siegel et al., 2017). According to the WHO Global Cancer Observatory (GLOBOCAN), 2018 Registry, lung cancer cases are the largest in the Cancer epidemic, with about 2 million cases (Mattiuzzi and Lippi, 2019). Although recent treatment advances have significant clinical impact in patients with lung cancer, but the side

effect still existed, some effect is not satisfactory (Mohindra and Patel, 2022). It is still vital to find new drugs and new treatment strategies for lung cancer.

Polysaccharides are large molecular compounds composed of multiple monosaccharide molecules and usually possess a complex structure. Due to their unique structure, polysaccharides usually have superior pharmacological applications, such as immunoregulatory, anti-tumor, anti-virus, antioxidation, and hypoglycemic activity (Yu et al., 2018), even the application for microencapsulation of probiotics (Liu et al., 2020), and therefore they play an important role in nature (Chen and Huang, 2018; Liu et al., 2020). In recent years, seaweed polysaccharides have been receiving widespread attention owing to their special biological activities, including anti-tumor activities, which have

\* Corresponding author.

\*\* Corresponding author.

E-mail addresses: [luolianxiang321@gdmu.edu.cn](mailto:luolianxiang321@gdmu.edu.cn) (L. Luo), [huangriming@scau.edu.cn](mailto:huangriming@scau.edu.cn) (R. Huang).

<sup>1</sup> These authors equally contributed to this work.

attracted wide attention in biochemistry and medicine (Florez et al., 2017; Zhao et al., 2020). Among them, the biological activities of *Spirulina* polysaccharides were particularly outstanding. Based on the research, PSP has anti-virus functions, enhancing immunity (Wu et al., 2016), anti-oxidation, anti-tumor, lowering blood sugar, and microbial-modulating activities (Matloub et al., 2013; Finamore et al., 2017). It was found that the water-soluble polysaccharide of *Spirulina* had anti-Hepatitis C virus, antioxidant, cytotoxic, and lipidemic activities (Matloub et al., 2013). *Spirulina* complex polysaccharide (CPS) has been researched and it contributed to down-regulating angiogenesis through Toll-like receptor 4 signaling to inhibit glioma growth (Kawanishi et al., 2013). A study aimed to determine a protective effect on dopaminergic neurons of the polysaccharide extracted from *Spirulina platensis*, and the results revealed that they had a protective effect on the damage of dopaminergic neurons, and the antioxidant properties of polysaccharides might be the basis of its neuroprotective effect (Zhang et al., 2015). Moreover, research also pointed that the polysaccharide extracted from *Spirulina platensis* evokes antitumor activity in gastric cancer cells via modulation of galectin-3 and exhibited cyto/DNA protection (Uppin et al., 2022). Otherwise, another research preliminarily talked that the polysaccharide from *Spirulina platensis* could remarkably inhibit the growth of A549 lung cancer cells but without the clear details of biological mechanism (Cai et al., 2022). Obviously, although there have been many studies on *Spirulina* polysaccharides, there was still a lack of research on *Spirulina* polysaccharides treating lung cancer, especially the potential mechanism. Therefore, it is important to deeply study *Spirulina* polysaccharides treating lung cancer.

To explore the effect of *Spirulina* polysaccharides on lung cancer, we extracted a *Spirulina* polysaccharide named PSP. The Lewis lung cancer-bearing mice were treated with PSP, and some apparent indicators such as tumor weight and tumor volume were measured. Furthermore, metabolic analysis and 16S rRNA sequencing was carried out in this research.

## 2. Materials and methods

### 2.1. Materials

Dried *Spirulina* powder (purchased from Foshan Lanqiang Biotechnology Co., Ltd.) was stored in the Guangdong Provincial Key Laboratory of Food Quality and Safety, South China Agricultural University (Guangzhou, China). Lewis lung cancer (LLC) cells and C57BL/6 female mice were purchased from the Guangdong Medical University (Guangzhou, China). Fetal bovine serum (FBS) was supplied by Gibco Life Technologies (Grand Island, NY, USA). Other mentioned chemical materials in this study were purchased from Guangzhou Chemical Co. LTD (Guangzhou, China). All the reagents used were of analytical grade.

### 2.2. Preparation of PSP

PSP was extracted by the method of the reports with some slight modifications (Song et al., 2019; Han et al., 2021). The dried *Spirulina* powder (100 g) was added to 2000 mL of water twice at 90 °C for 2 h. Then the filtrate was concentrated to a quarter of the original volume by rotary evaporation at 52 °C. After centrifugation, the supernatant was mixed with triploid anhydrous ethanol for overnight precipitation to get the precipitate. The precipitate was dissolved in distilled water and then deproteinated by Sevag reagent (CHCl<sub>3</sub>: n-C<sub>4</sub>H<sub>9</sub>OH = 4:1, v/v). The protein-free polysaccharide solution was dialyzed in distilled water for three days. The cut-off molecular weight of the dialysis bag is 3000 Da. Finally, PSP was obtained after lyophilizing the dialysate. The total sugar content, protein content, relative molecular weight, monosaccharide composition, and functional groups of PSP were measured (Hao et al., 2019; Song et al., 2020). These results are shown in Tables S1–S2 and Fig. S1.

### 2.3. Animal experiment

$5 \times 10^5$  LLC cells were resuspended in a free FBS medium and injected subcutaneously in a 100  $\mu$ L volume into the right flank of 8-week-C57BL/6 female mice. After the tumor grew to about approximately 60 mm<sup>3</sup>, the mice were divided into two groups (five mice per group). The vehicle group was treated with vehicle and the PSP group was treated with PSP (200 mg/kg) via intragastric administration daily for 15 days. The mice's body weights were recorded every day, and the signs of toxicity were monitored. The tumors of the mice were measured with a digital caliper every three days. The tumor volumes were calculated by the following formula:

$$\text{volume (mm}^3\text{)} = \text{length (mm)} \times \text{width (mm)}^2 / 2$$

### 2.4. Metabolomic analysis

The metabolic analysis is carried out according to the reported methods (Xia et al., 2021). In short, the cell sample stored at –80 °C refrigerator was thawed on ice. Each sample was taken 50 mg and added to 1 mL icy methanol/water (70%, v/v) to homogenize and vortexed for 3 min. The sample was centrifuged (4 °C, 12000 rpm, 15 min), then collected and desiccated in a centrifuge. Then, 200  $\mu$ L aliquots of supernatant were transferred for LC-MS/MS analysis. The samples of quality control (QC) were performed by mixing 10  $\mu$ L of every single sample, then researching the other samples to control the reproducibility of instrumental research. And, an ACQUIY UPLC BEH column (2.1 mm  $\times$  100 mm, 1.7  $\mu$ m, waters, Ireland) was used to analyze the samples for separation. 25 mM ammonium hydroxide and 25 mM ammonium acetate in water (A) and acetonitrile (B) were performed as the mobile phase in both electrospray ionization (ESI) positive patterns (5500V) and negative patterns (–4500V).

### 2.5. Microbial analysis

Based on 16S rRNA sequencing, microbial analysis was carried out according to the reported methods (Abd-Elaziz et al., 2020). DNA was extracted based on the instructions of the Omega Kit e.z.n.a TM Mag-Bind SOIL DNA Kit (<http://omegabiotek.com/store/product/soil-dna-kit/>). Before the experiment, DNA integrity was measured through an agarose gel. Primers were used to amplify the v3-v4 region of the microbial 16S ribosomal gene. The primers were 341F (5'-CCTAC GGGNGGCWGCAG-3') and 805R (5'-GACTACHVGGGTATCTAAT CC-3'). Two rounds of PCR amplification were conducted. The first round of amplification was carried out under the following conditions: 94 °C for 3 min, 5 cycles at 94 °C for 30 s, 45 °C for 20 s, 65 °C for 30 s, and then 20 cycles at 94 °C for 20 s, 55 °C for 20 s, 72 °C for 30 s and finally extending at 72 °C for 5 min. After amplification, PCR primers from the first round were introduced into the Illumina Bridge PCR compatible primers for the second round of amplification. Reaction conditions of the second amplification were as follows: 94 °C for 3 min, 5 cycles at 94 °C for 20 s, 55 °C for 20 s, 72 °C for 30 s and finally extending at 72 °C for 5 min. After amplification, the PCR products were detected using agarose electrophoresis to purify and recover the DNA. The recovered DNA was quantified accurately by the Qubit3.0 DNA detection kit and mixed in an equal amount of 1:1 to facilitate the sequencing.

### 2.6. Statistical analysis

Data were shown as mean average  $\pm$  standard deviations (SD) (n = 3). Data in all the bioassays were evaluated by Student's t-test at a univariate level, p-value < 0.05 or p-value < 0.01 were respectively regarded as significant differences or extremely significant differences. \*\*p < 0.01, \*\*\*p < 0.001 as compared to control sample. The online Kyoto Encyclopedia of Genes and Genomes (KEGG, <http://www.kegg>.

jp/) was used to query and map the KEGG pathways and the DAMs.

### 3. Results and discussion

#### 3.1. PSP on tumor volume and tumor weight in lung cancer-bearing mice

We first established a lung cancer mouse model to demonstrate whether PSP inhibited tumor growth. As shown in Fig. 1A, tumors in the *Spirulina* polysaccharide (SPI) group were significantly smaller than in the Vehicle group. Within 15 days, tumor volume increased gradually in the Vehicle group but not in the SPI group. On day 15, there was a significant difference in tumor volume between the two groups ( $p < 0.001$ ), which was statistically significant (Fig. 1B). In addition, there were also significant differences in tumor weight between the two groups ( $p < 0.01$ ) (Fig. 1C). According to the result, we speculated that PSP had an inhibitory effect on lung cancer.

#### 3.2. Metabolomics analysis

To explore changes in tumor metabolites, we performed metabolomics analyses on the tumors of treated and control mice. A total of 27 DAMs were screened, among which 24 DAMs were up-regulated while 3 DAMs were down-regulated. To see the differences in metabolites more intuitively, we drew a differential metabolite volcano plot (Fig. 2A). 27 DAMs were grouped into different categories. As shown in Fig. 2B, these DAMs were mainly oxidized lipid and organic acid and its derivatives.

KEGG enrichment results were shown in Fig. 2C–D. Among the enriched pathways, Fructose and mannose metabolism, FcεRI signaling pathway, and arachidonic acid metabolism are highly enriched with the  $p$ -value under 0.05. In Fructose and mannose metabolism, L-fucose and L-rhamnose were significantly increased. Since both L-fucose and L-rhamnose are the main components of PSP, it was reasonable to believe that their significant upregulation of them was due to the intake of PSP. The other two significantly enriched pathways may be related to the anticancer activity of PSP. Consequently, there is a strong relationship between the two pathways.

FcεRI signaling pathway is closely related to immunity. IgE binds to the IgE receptor is the FcεRI and a member of the antigen receptor superfamily and is generally expressed on eosinophils and mast cells. It plays a vital role in connecting pathogen or antigen-specific IgE and cellular immune effector function (Berings et al., 2018). FcεRI, which activates eosinophils or mast cells to release and secrete mediators such as histamine, heparin, proteinoids, and metabolites of arachidonic acid, cytokines, and so on (Olivera et al., 2018). After being activated, eosinophils or mast cells play their biological roles mainly through releasing and secreting mediators. When eosinophils or mast cells are activated, mediators released into the extracellular environment participate in the inflammatory response, significantly impacting the body (Lu et al., 2011). Arachidonic acid metabolism was a downstream pathway of the FcεRI signaling pathway. In this pathway, arachidonic

acid does not exist free in cells but is esterified in the cell membrane as a phospholipid. When stimulated, the arachidonic acid is dissociated by phospholipase and converted into active metabolites under the action of various arachidonic acid metabolic enzymes, such as Leukotrienes (LTs) (Hanna and Hafez, 2018). LTs are a class of highly bioactive arachidonic acid derivatives. They can directly or indirectly promote innate immune response by affecting leukocyte effector function (Nicolette et al., 2008), stimulating the production of other inflammatory mediators (Liu and Yokomizo, 2015), inducing phagocytosis (Zhang et al., 2017), and activating antimicrobial mechanisms (Yokomizo et al., 2018). In this study, the FcεRI signaling pathway and arachidonic acid metabolism both enriched significantly. Leukotriene D4 (LTD<sub>4</sub>) and leukotriene E4 (LTE<sub>4</sub>) were significantly up-regulated in the FcεRI signaling pathway, while leukotriene B4 (LTB<sub>4</sub>), LTD<sub>4</sub>, and LTE<sub>4</sub> were significantly up-regulated in arachidonic acid metabolism. LTB<sub>4</sub> is a strong pro-inflammatory factor, which can increase vascular permeability, induce the release of lysosomal enzymes, promote the production of reactive oxygen species and enhance the expression of TNF-α, IL-1, IL-6, IL-2 (Laye et al., 2018). LTD<sub>4</sub> and LTE<sub>4</sub> can enhance the posterior venules' plasma penetration and mucus secretion in the inflammatory process and regulate the Th2 cell-dependent pneumonia response (Austen, 2007).

Based on the metabolomics analysis results, it can be speculated that B lymphocytes transform into plasma cells and produce IgE in response to PSP stimulation. IgE then binds to FcεRI on eosinophils or mast cells to activate eosinophils or mast cells, thereby activating the arachidonic acid pathway. Arachidonic acid was free from the cell membrane. Then, 5-lipoxygenase (5-LOX) catalyzed the transformation of arachidonic acid into Leukotriene A4 (LTA<sub>4</sub>) with the assistance of 5-LOX activated proteins. Due to the instability of LTA<sub>4</sub>, LTA<sub>4</sub> was catalyzed by epoxide hydrolase (LTA4H) to produce LTB<sub>4</sub> or combined with glutathione to transform into LTC<sub>4</sub>. LTB<sub>4</sub> and LTC<sub>4</sub> are subsequently transported extracellularly and lysed into LTD<sub>4</sub> and LTE<sub>4</sub> (Tian et al., 2020). Therefore, LTB<sub>4</sub>, LTD<sub>4</sub>, and LTE<sub>4</sub> were significantly increased. As critical inflammatory mediators, LTB<sub>4</sub>, LTE<sub>4</sub>, and LTD<sub>4</sub> participate in inflammatory responses by stimulating mucus secretion (Otaka et al., 2019), increasing vascular permeability (Papadaki et al., 2013), and causing smooth muscle contraction (Bonvini et al., 2020), thus influencing tumor development (Fig. 3).

#### 3.3. PSP on gut microbiota in lung cancer-bearing mice

A total of 6136 operational taxonomic units (OTUs) were detected at a similar level of 97% in the sequencing. There are 2096 OTUs overlaps between the Vehicle group and SPI group (Fig. 4A). In this study, we reflect the abundance and diversity of microbial communities through a single-sample diversity analysis (Alpha diversity). According to the sequencing results (Fig. 4B), compared with the Vehicle group, all the indexes, including Shannon, Simpson, Chao, and ACE, decreased in the SPI group. Although the Alpha index between the two groups showed no

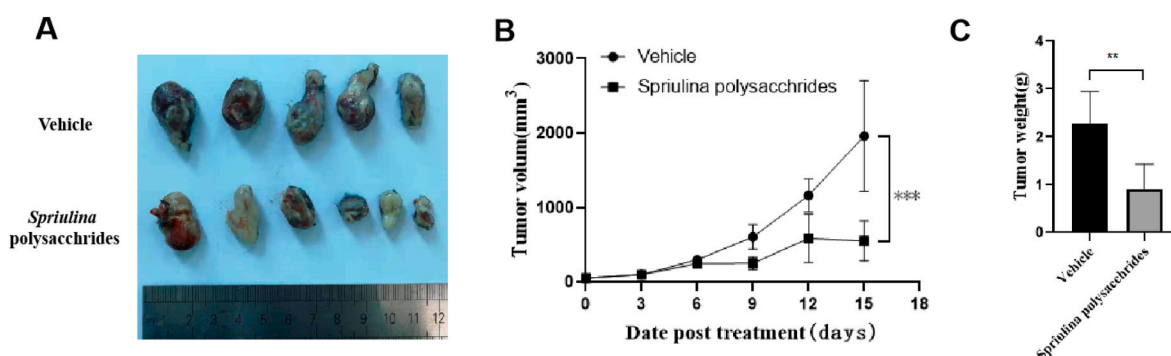


Fig. 1. (A) Tumor size comparison between the SPI group and Vehicle group. (B) Tumor volume. (C) Tumor weight. \*\* $p < 0.01$ , \*\*\* $p < 0.001$ .

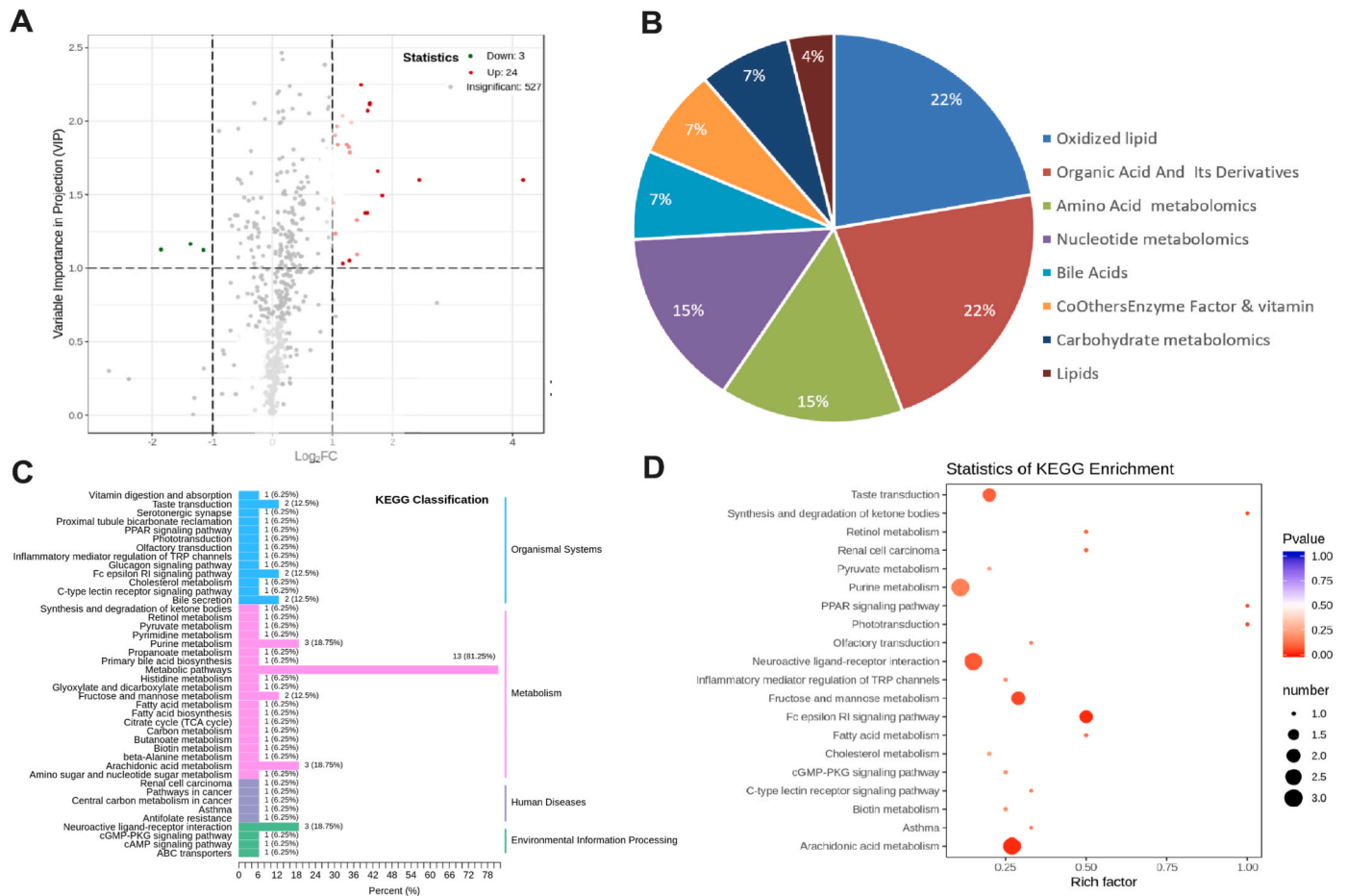


Fig. 2. (A) Volcanic plot. (B) Proportion diagram of DAMs classification. (C) KEGG classification map. (D) KEGG enrichment map.

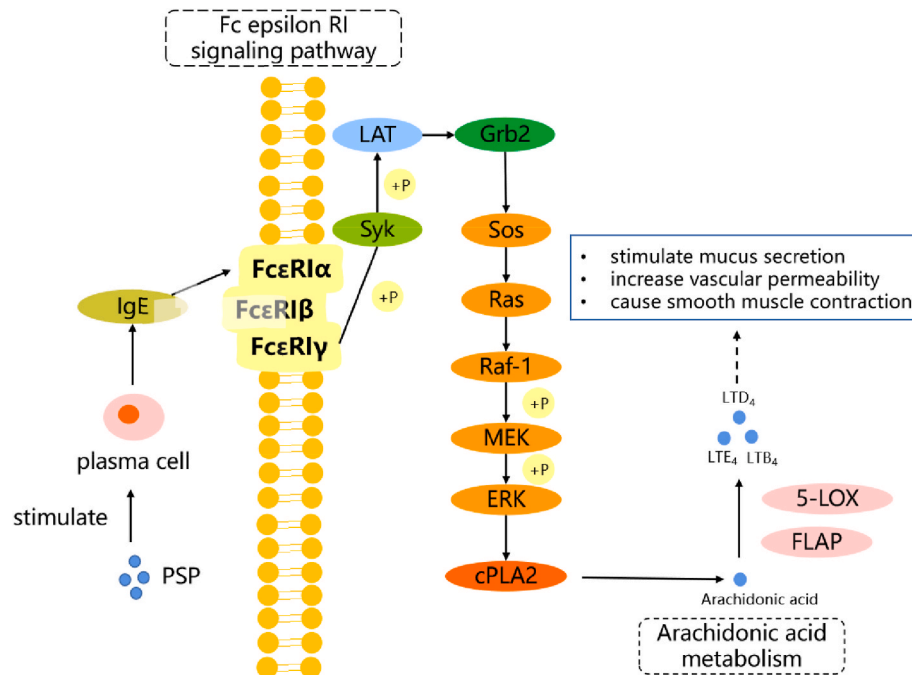


Fig. 3. Diagram of the potential pathways of PSP against lung cancer. Syk: Spleen tyrosine kinase; LAT: Linker for activation of T cells; Grb2: Growth factor receptor-bound protein 2; Sos: Son of sevenless; Ras: GTPase HRas; Raf-1: RAF proto-oncogene serine; MEK: Mitogen-activated protein kinase kinase 1; ERK: Mitogen-activated protein kinase 1/3; cPLA2: Cytosolic phospholipase A2; FLAP: Arachidonate 5-lipoxygenase-activating protein.



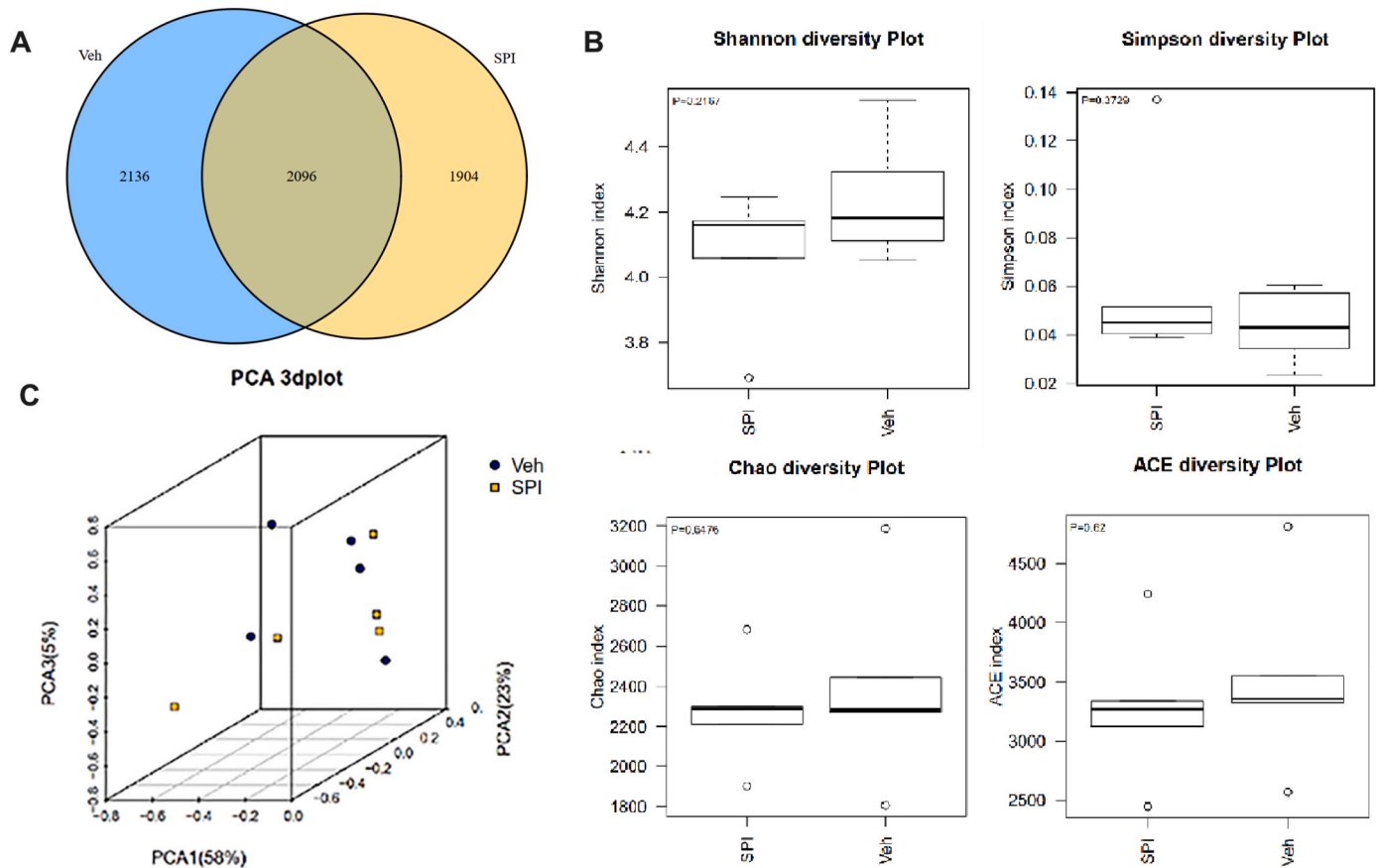


Fig. 4. (A) The Wayne diagram of OTUs sample distribution. (B) Box graph of Alpha index between the SPI group and Vehicle group. (C) PCA 3D diagram based on OTUs. (D) Distribution bar plot of the community structure at the phylum level. (E) Stack bar chart of species abundance at the phylum level. (F) The proportions of the four dominant gates in the SPI and Vehicle group. (G) Error plot of difference comparison between SPI group and Vehicle group at the genus level. (H) Visualization of classification and phylogenetic information. Phyla corresponding to the top 20 abundance species (marked with an asterisk) are colored differently. The size of circles and asterisks represents the difference in abundance. (I) Linear discriminant analysis bar chart. (J) Linear discriminant analysis diagram.

significant difference, PCA analysis results still showed differences between the two groups (Fig. 4C).

PSP significantly altered the gut microbiota structure in tumor mice. Based on the results, there were four dominant phyla: *Firmicutes*, *Bacteroidetes*, *Actinobacteria*, and *Proteobacteria* (Fig. 4D). The four dominant phyla showed changes in abundance. Compared with the Vehicle group, the abundance of *Firmicutes* and *Actinobacteria* in the SPI group increased while *Bacteroidetes* and *Proteobacteria* decreased (Fig. 4E). According to the data in Fig. 4F, the gut microbiota, *Firmicutes/Bacteroidetes* ratio (F/B) was increased under the PSP treatment. *Firmicutes* and *Bacteroidetes* are the two main phyla of gut microbiota, and the F/B value is mainly related to maintaining the balance of gut microbiota (Grigor'eva, 2021). A high F/B value can lead to obesity (Abenavoli et al., 2019), while a low F/B value leads to inflammatory bowel disease (Shen et al., 2018). In our study, the PSP treatment increased the F/B value and made the F/B value more toward 1. These results suggested that PSP could contribute to regulating the balance of gut microbiota to maintain intestinal homeostasis.

As shown in Fig. 4G, the abundance of *Turicibacter* in *Firmicutes* increased ( $p = 0.016$ ), while the abundance of *Desulfovibrio* ( $p = 0.058$ ) in *Proteobacteria* decreased. The abundance of *Bifidobacterium* ( $p = 0.059$ ) in *Actinobacteria* and *Alloprevotella* ( $p = 0.097$ ) in *Bacteroidetes* increased. According to the classification comparison results, we selected the classification of dominant species and drew a circular tree diagram combining the species abundance information (Fig. 4H). According to the changes in the genera level community, PSP treatment could increase the abundance of some beneficial bacteria such as

*Allobaculum*, *Lactobacillus*, *Alloprevotella*, and *Olsenella*. Meanwhile, it reduced the abundance of some conditional pathogenic bacteria, such as *Bacteroides* and *Acinetobacter* (Qin, 2019). Therefore, we speculated that PSP exerted its activity by changing the abundance and composition of beneficial bacteria and pathogenic bacteria in the gut microbiota.

We obtained critical gut microbes through LefSe analysis. The results were shown below (Fig. 4I–J). *Desulfovibrionaceae*, *Deltaproteobacteria*, and *Desulfovibrionales* in the Vehicle group showed selective enrichment. In contrast, *Bifidobacteriaceae*, *Bifidobacteriales*, *Bifidobacterium*, and *Turicibacter* increased in the SPI group. As an essential probiotic in the human body, *Bifidobacterium* plays a vital role in human health. By metabolizing organic acids and other antibacterial active substances, *Bifidobacterium* inhibits the proliferation or infection of harmful bacteria and pathogenic bacteria to change the physical and chemical characteristics of the intestine and finally achieves the goal of inhibiting the production of carcinogens (Feng et al., 2019). Some *Turicibacter* bacteria were associated with inflammation in the host (Kellermayer et al., 2011). The *Desulfovibrion* family, a kind of sulfate-reducing bacteria, can produce  $H_2S$  (Peck et al., 2019), which may be associated with cancer such as the colorectal cancer (Guo et al., 2016). Excessive  $H_2S$  is harmful to the colon epithelium's energy metabolism and DNA integrity (Beaumont et al., 2016). *Deltaproteobacteria* is one of the classes of *Proteobacteria* and may be related to the occurrence of the inflammatory intestinal disorder (Wang et al., 2009). LefSe analysis results led us to speculate that the increase in the abundance of *Bifidobacteria* and the decrease of some *Proteobacteria* might be related to the inhibition of lung cancer by PSP.

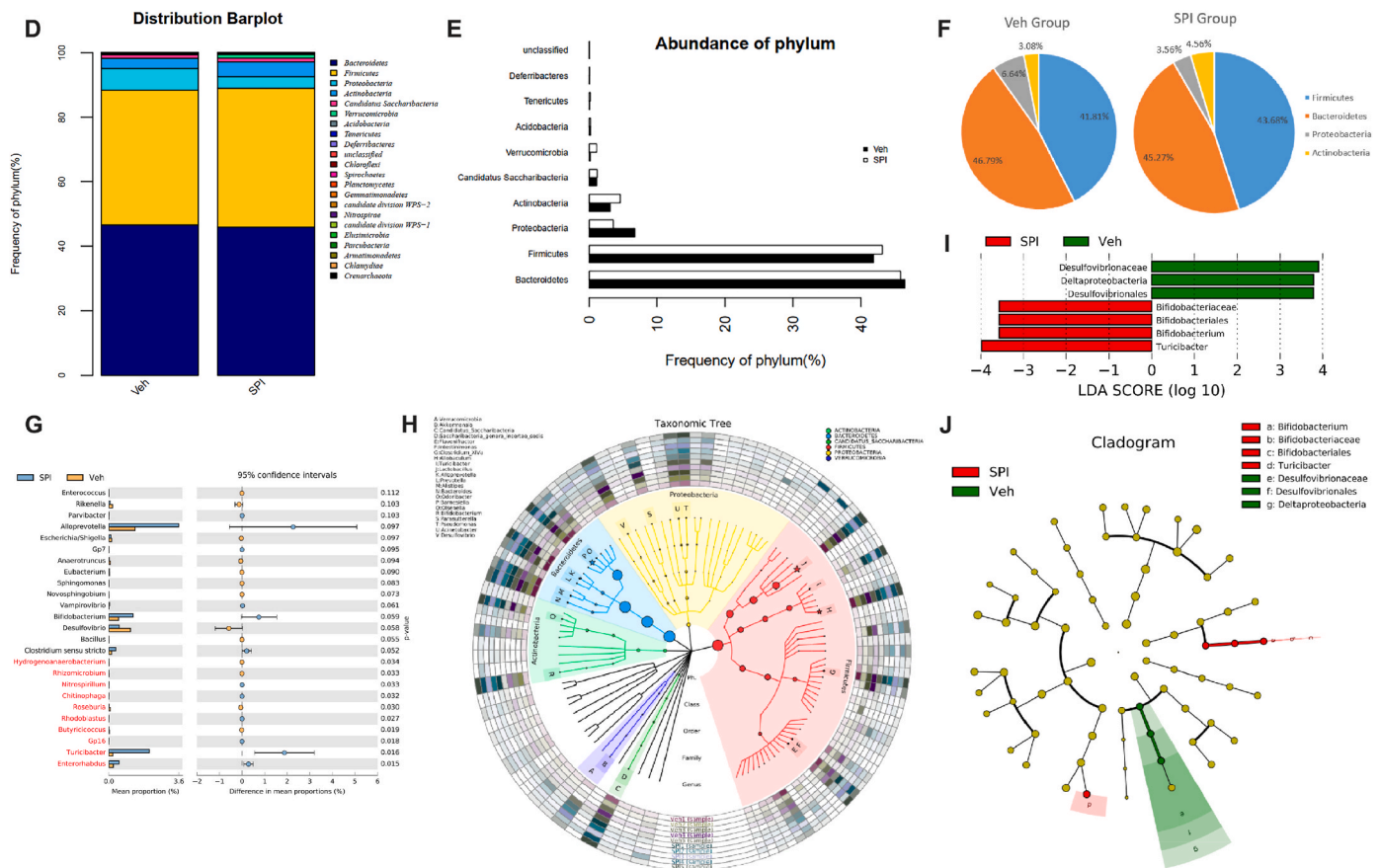


Fig. 4. (continued).

4. Conclusion

In this study, we first studied the apparent effects of PSP on tumors in LLC tumor-bearing mice. Then we elucidated the effects of PSP on tumor metabolism and gut microbiota. According to the results, we could see that the tumor volume decreased significantly after PSP treatment. Based on the metabolomic analysis, the LTB<sub>4</sub>, LTD<sub>4</sub>, and LTE<sub>4</sub> showed a significant increase, and they were both involved in the FcεRI signaling pathway and arachidonic acid metabolism pathway, which were the two significantly enriched pathways in KEGG pathway enrichment. 16S rRNA sequencing results showed an increase in some beneficial bacteria such as *Bifidobacterium*, *Lactobacillus*, *Allobaculum*, and *Alloprevotella*. In contrast, some conditional pathogenic bacteria, such as *Bacteroides* and *Acinetobacter*, were down-regulated, suggesting that PSP might maintain intestinal homeostasis by altering the abundance of probiotics and harmful bacteria in the gut microbiota to achieve anti-tumor goals. This study provides a basic investigation of new potential molecular mechanisms of PSP on lung cancer, including the tumor metabolism and gut microbiota, our results may contribute to a deeper development of PSP and the research of biological treatment on lung cancer. However, further research is still required to obtain a deeper understanding of this research.

Ethics statements

This study includes animal experiments. The animal experiments involved were conducted through the Animal Ethics Committee of Guangdong Medical University (No.110324210104725223, animal experiments were performed in compliance with institutional animal care guidelines and according to committee-approved protocols).

CRediT authorship contribution statement

**Yingfang Lu:** Methodology, Writing – original draft. **Bo Peng:** Resources, Writing – original draft. **Yuqi Lin:** Writing – original draft, Data curation. **Qianmin Lin:** Data curation. **Xuwei Xia:** Data curation. **Saiyi Zhong:** Writing – review & editing, Supervision. **Lianxiang Luo:** Methodology, Visualization. **Riming Huang:** Conceptualization, Methodology, Funding acquisition.

Declaration of competing interest

The authors declare that they have no known competing financial interests or personal relationships that could have appeared to influence the work reported in this paper.

Acknowledgments

This work was financially supported by the Program of Department of Natural Resources of Guangdong Province (No. GDNRC[2021]53), the National Natural Science Foundation of China (No. 32161160304), Key-Area Research and Development Program of Guangdong Province (No.2020B1111030004), Guangdong Provincial Key Laboratory of Aquatic Product Processing and Safety (No. GDPKLAPPS2102), and the Innovative Team Program of High Education of Guangdong Province (No. 2021KCXTD021).

Appendix A. Supplementary data

Supplementary data to this article can be found online at <https://doi.org/10.1016/j.crfs.2022.08.010>.

## References

- Abd-Elaziz, A.M., Karam, E.A., Ghanem, M.M., Moharam, M.E., Kansoh, A.L., 2020. Production of a novel alpha-amylase by *Bacillus atrophaeus nrc1* isolated from honey: purification and characterization. *Int. J. Biol. Macromol.* 148, 292–301.
- Abenavoli, L.E., Scarpellini, C., Colica, L., Boccuto, B., Salehi, J., Sharifi-Rad, V., Aiello, B., Romano, A., De Lorenzo, A.A., Izzo and R., Capasso, 2019. Gut microbiota and obesity: a role for probiotics. *Nutrients* 11 (11).
- Austen, K.F., 2007. Additional functions for the cysteinyl leukotrienes recognized through studies of inflammatory processes in null strains. *Prostag. Other Lipid Mediat.* 83 (3), 182–187.
- Beaumont, M., Andriamihaja, M., Lan, A., Khodorova, N., Audebert, M., Blouin, J.M., Grauso, M., Lancha, L., Benetti, P.H., Benamouzig, R., Tome, D., Bouillaud, F., Davila, A.M., Blachier, F., 2016. Detrimental effects for colonocytes of an increased exposure to luminal hydrogen sulfide: the adaptive response. *Free Radic. Biol. Med.* 93, 155–164.
- Berings, M., Gevaert, P., De Ruycq, N., Derycke, L., Holtappels, G., Pilette, C., Bachert, C., Lambrecht, B.N., Dullaers, M., 2018. Fc epsilon RI expression and Ige binding by dendritic cells and basophils in allergic rhinitis and upon allergen immunotherapy. *Clin. Exp. Allergy* 48 (8), 970–980.
- Bonvini, S.J., Birrell, M.A., Dubuis, E., Adcock, J.J., Wortley, M.A., Flajolet, P., Bradding, P., Belvisi, M.G., 2020. Novel airway smooth muscle-mast cell interactions and a role for the trpv4-atp axis in non-atopic asthma. *Eur. Respir. J.* 56 (1).
- Bray, F., Ferlay, J., Soerjomataram, I., Siegel, R.L., Torre, L.A., Jemal, A., 2018. Global cancer statistics 2018: globocan estimates of incidence and mortality worldwide for 36 cancers in 185 countries. *CA A Cancer J. Clin.* 68 (6), 394–424.
- Cai, B., Zhao, X., Luo, L., Wan, P., Chen, H., Pan, J., 2022. Structural characterization, and in vitro immunostimulatory and antitumor activity of an acid polysaccharide from *Spirulina platensis*. *Int. J. Biol. Macromol.* 196, 46–53.
- Chen, L., Huang, G.L., 2018. Antitumor activity of polysaccharides: an overview. *Curr. Drug Targets* 19 (1), 89–96.
- Feng, Y.Q., Duan, Y.F., Xu, Z.J., Lyu, N., Liu, F., Liang, S.H., Zhu, B.L., 2019. An examination of data from the American Gut Project reveals that the dominance of the genus *Bifidobacterium* is associated with the diversity and robustness of the gut microbiota. *Microbiol. Open* 8 (12).
- Finamore, A., Palmery, M., Bensehaila, S., Peluso, I., 2017. Antioxidant, immunomodulating, and microbial-modulating activities of the sustainable and ecofriendly *Spirulina*. *Oxid. Med. Cell. Longev.*, 3247528, 2017.
- Florez, N., Gonzalez-Munoz, M.J., Ribeiro, D., Fernandes, E., Dominguez, H., Freitas, M., 2017. Algae polysaccharides' chemical characterization and their role in the inflammatory process. *Curr. Med. Chem.* 24 (2), 149–175.
- Grigor'eva, I.N., 2021. Gallstone disease, obesity and the Firmicutes/Bacteroidetes ratio as a possible biomarker of gut dysbiosis. *J. Personalized Med.* 11 (1), 13.
- Guo, F.F., Yu, T.C., Hong, J., Fang, J.Y., 2016. Emerging roles of hydrogen sulfide in inflammatory and neoplastic colonic diseases. *Front. Physiol.* 7.
- Han, Y., Wu, Y., Li, G., Li, M., Yan, R., Xu, Z., Lei, H., Sun, Y., Duan, X., Hu, L., Huang, R., 2021. Structural characterization and transcript-metabolite correlation network of immunostimulatory effects of sulfated polysaccharides from green *Alga ulva pertusa*. *Food Chem.* 342.
- Hanna, V.S., Hafez, E.A.A., 2018. Synopsis of arachidonic acid metabolism: a review. *J. Adv. Res.* 11, 23–32.
- Hao, H.L., Han, Y., Yang, L.H., Hu, L.M., Duan, X.W., Yang, X., Huang, R.M., 2019. Structural characterization and immunostimulatory activity of a novel polysaccharide from green *Alga caulerpa racemosa var peltata*. *Int. J. Biol. Macromol.* 134, 891–900.
- Kawanishi, Y., Tominaga, A., Okuyama, H., Fukuoka, S., Taguchi, T., Kusumoto, Y., Yawata, T., Fujimoto, Y., Ono, S., Shimizu, K., 2013. Regulatory effects of *Spirulina* complex polysaccharides on growth of murine rsv-m glioma cells through toll-like receptor 4. *Microbiol. Immunol.* 57 (1), 63–73.
- Kellermayer, R., Dowd, S.E., Harris, R.A., Balasa, A., Schaible, T.D., Wolcott, R.D., Tatevian, N., Szigeti, R., Li, Z.J., Versalovic, J., Smith, C.W., 2011. Colonic mucosal DNA methylation, immune response, and microbiome patterns in toll-like receptor 2-knockout mice. *Faseb. J.* 25 (5), 1449–1460.
- Laye, S., Nadjar, A., Joffre, C., Bazinet, R.P., 2018. Anti-inflammatory effects of omega-3 fatty acids in the brain: physiological mechanisms and relevance to pharmacology. *Pharmacol. Rev.* 70 (1), 12–38.
- Liu, M., Yokomizo, T., 2015. The role of leukotrienes in allergic diseases. *Allergol. Int.* 64 (1), 17–26.
- Liu, H., Xie, M., Nie, S., 2020. Recent trends and applications of polysaccharides for microencapsulation of probiotics. *Food Frontiers* 1 (1), 45–59.
- Lu, Y., Yang, J.H., Li, X., Hwangbo, K., Hwang, S.L., Taketomi, Y., Murakami, M., Chang, Y.C., Kim, C.H., Son, J.K., Chang, H.W., 2011. Emodin, a naturally occurring anthraquinone derivative, suppresses Ige-mediated anaphylactic reaction and mast cell activation. *Biochem. Pharmacol.* 82 (11), 1700–1708.
- Matloub, A.A., El-Senousy, W.M., Elsayed, A.B., ElSouda, S., Aly, H., 2013. Anti-hcv, antioxidant, cytotoxic and hypolipidemic activities of water soluble polysaccharides of *Spirulina platensis*. *Planta Med.* 79 (13), 1159–1159.
- Mattiuzzi, C., Lippi, G., 2019. Current cancer epidemiology. *J. Epidemiol. Glob. Health.* 9 (4), 217–222.
- Mohindra, N.A., Patel, J.D., 2022. Top Advances in Lung Cancer. *Cancer*, 2021.
- Nicolette, R., Rius, C., Piqueras, L., Jose, P.J., Sorgi, C.A., Soares, E.G., Sanz, M.J., Faccioli, L.H., 2008. Leukotriene b4-loaded microspheres: a new therapeutic strategy to modulate cell activation. *BMC Immunol.* 9.
- Olivera, A., Beaven, M.A., Metcalfe, D.D., 2018. Mast cells signal their importance in health and disease. *J. Allergy Clin. Immunol.* 142 (2), 381–393.
- Otaka, J.N.P., Toledo, L.F.A., Silva, K.M., Silva, A.A., Agra, L., Diaz, B.L., Lessa, D.A.B., 2019. Leukotriene b4 in equine asthma syndrome: what do we know so far? *Pesqui. Vet. Bras.* 39 (9), 723–727.
- Papadaki, G., Bakalos, P., Kostikas, K., Hillas, G., Tsiligianni, Z., Koulouris, N.G., Papiiris, S., Loukides, S., 2013. Vascular endothelial growth factor and cysteinyl leukotrienes in sputum supernatant of patients with asthma. *Respir. Med.* 107 (9), 1339–1345.
- Peck, S.C., Denger, K., Burrichter, A., Irwin, S.M., Balskus, E.P., Schleheck, D., 2019. A glycol radical enzyme enables hydrogen sulfide production by the human intestinal bacterium *Bifidobacterium wadsworthia*. *P Natl Acad Sci USA* 116 (8), 3171–3176.
- Shen, Z.H., Zhu, C.X., Quan, Y.S., Yang, Z.Y., Wu, S., Luo, W.W., Tan, B., Wang, X.Y., 2018. Relationship between intestinal microbiota and ulcerative colitis: mechanisms and clinical application of probiotics and fecal microbiota transplantation. *World J. Gastroenterol.* 24 (1), 5–14.
- Siegel, R.L., Miller, K.D., Jemal, A., 2017. Cancer statistics, 2017. *CA A Cancer J. Clin.* 67 (1), 7–30.
- Siegel, R.L., Miller, K.D., Jemal, A., 2019. Cancer statistics, 2019. *CA A Cancer J. Clin.* 69 (1), 7–34.
- Song, Y., Zhu, M., Hao, H., Deng, J., Li, M., Sun, Y., Yang, R., Wang, H., Huang, R., 2019. Structure characterization of a novel polysaccharide from Chinese wild fruits (*Passiflora foetida*) and its immune-enhancing activity. *Int. J. Biol. Macromol.* 136, 324–331.
- Song, Y., Wen, P., Hao, H., Zhu, M., Sun, Y., Zou, Y., Requena, T., Huang, R., Wang, H., 2020. Structural features of three hetero-galacturonans from *Passiflora foetida* fruits and their in vitro immunomodulatory effects. *Polymers* 12 (3).
- Tian, W., Jiang, X.G., Kim, D., Guan, T., Nicolls, M.R., Rockson, S.G., 2020. Leukotrienes in tumor-associated inflammation. *Front. Pharmacol.* 11.
- Uppin, V., Dharmesh, S.M., R, S., 2022. Polysaccharide from *Spirulina platensis* evokes antitumor activity in gastric cancer cells via modulation of galectin-3 and exhibited cyto/DNA protection: structure-function study. *J. Agric. Food Chem.* 70 (23), 7058–7069.
- Wang, Y.W., Hoenig, J.D., Malin, K.J., Qamar, S., Petrof, E.O., Sun, J., Antonopoulos, D.A., Chang, E.B., Claud, E.C., 2009. 16s rRNA gene-based analysis of fecal microbiota from preterm infants with and without necrotizing enterocolitis. *ISME J.* 3 (8), 944–954.
- Wu, Q.H., Liu, L., Miron, A., Klimova, B., Wan, D., Kuca, K., 2016. The antioxidant, immunomodulatory, and anti-inflammatory activities of *Spirulina*: an overview. *Arch. Toxicol.* 90 (8), 1817–1840.
- Xia, X.W., Hao, H.L., Zhang, X.Y., Wong, I.N., Chung, S.K., Chen, Z.X., Xu, B.J., Huang, R.M., 2021. Immunomodulatory sulfated polysaccharides from *Caulerpa racemosa var. peltata* induces metabolic shifts in nf-kb signaling pathway in raw 264.7 macrophages. *Int. J. Biol. Macromol.* 182, 321–332.
- Yokomizo, T., Nakamura, M., Shimizu, T., 2018. Leukotriene receptors as potential therapeutic targets. *J. Clin. Invest.* 128 (7), 2691–2701.
- Yu, Y., Shen, M., Song, Q., Xie, J., 2018. Biological activities and pharmaceutical applications of polysaccharide from natural resources: a review. *Carbohydr. Polym.* 183, 91–101.
- Zhang, F., Lu, J., Zhang, J.G., Xie, J.X., 2015. Protective effects of a polysaccharide from *Spirulina platensis* on dopaminergic neurons in an mptp-induced Parkinson's disease model in c57bl/6j mice. *Neural Regen. Res.* 10 (2), 308–313.
- Zhang, Y., Olson, R.M., Brown, C.R., 2017. Macrophage Itb4 drives efficient phagocytosis of *Borrelia burgdorferi* via btl1 or btl2. *J. Lipid Res.* 58 (3), 494–503.
- Zhao, C., Lin, G., Wu, D., Liu, D., You, L., Högger, P., Simal-Gandara, J., Wang, M., da Costa, J.G.M., Marunaka, Y., Daglia, M., Khan, H., Filosa, R., Wang, S., Xiao, J., 2020. The algal polysaccharide ulvan suppresses growth of hepatoma cells. *Food Frontiers* 1 (1), 83–101.